

DOI: 10.1002/cctc.201200311

Low-Temperature Chemoselective Gold-Surface-Mediated Hydrogenation of Acetone and Propionaldehyde

Ming Pan,^[a] Zachary D. Pozun,^[b] Adrian J. Brush,^[a] Graeme Henkelman,^[b] and C. Buddie Mullins^{*[a]}

Since nanoscale gold was first discovered to be catalytically active,^[1] gold-based catalysts have been studied both theoretically^[2] and experimentally^[3] in a wide range of reactions.^[4] These catalysts exhibit high activity for hydrogenation processes,^[5] in particular showing enhanced selectivity.^[6] However, there is a lack of relevant fundamental studies into these processes. Conducting hydrogenation reactions on model gold surfaces is useful for obtaining mechanistic insight and for further enhancing our understanding of the catalytic properties of supported-gold catalysts. Herein, we report the chemoselective hydrogenation of aldehydes over ketones on gold surfaces.

The hydrogenation chemistry of oxygenated hydrocarbons has been studied on transition-metal surfaces for a variety of reactions that are important to the pharmaceutical- and chemical industries.^[7] For example, C=O bond hydrogenation is a key step in the catalytic conversion of cellulosic biomass.^[8] In addition, gold-based catalysts have also shown exceptional activity for the selective hydrogenation of α,β -unsaturated carbonyl compounds.^[9] Claus found that, in the production of allyl alcohol from the hydrogenation of acrolein, gold catalysts yielded about 10-times-higher selectivity for C=O bond hydrogenation than traditional platinum-based catalysts.^[10] Therefore, exploring the individual reactivity of carbonyl-hydrogenation could provide useful information for a better holistic understanding of these important catalytic reactions.

By employing propionaldehyde and acetone as representative probe molecules of aldehydes and ketones, respectively, we investigated the hydrogenation of C=O bonds on a model pre-atomic-hydrogen-covered Au(111) catalyst. H atoms were used herein owing to the high energetic barrier of H₂-dissociation on gold.^[11] Temperature-programmed-desorption (TPD) measurements indicated different activities for hydrogenation on gold: propionaldehyde underwent hydrogenation to afford 1-propanol on H-covered gold but acetone did not form 2-propanol. Density functional theory (DFT) calculations revealed different activation energies for the reactions between a single carbonyl moiety and a H atom.

First, the hydrogenation of acetone was investigated on a Au(111) surface. In a control experiment (Figure 1 a), 1.62 ML (ML=monolayer) of acetone ($m/z=43$, the most-abundant mass fragment of acetone) was adsorbed onto a clean Au(111)

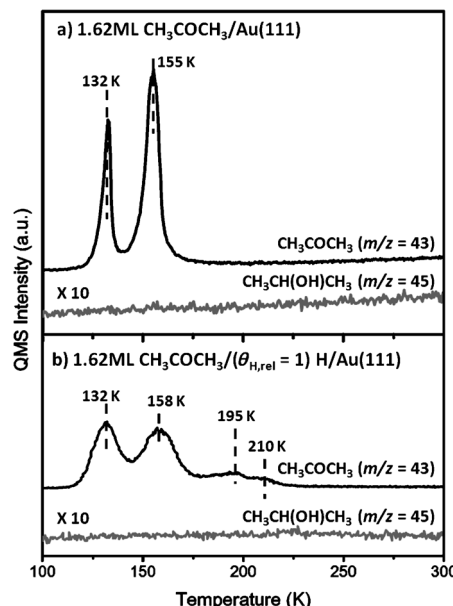


Figure 1. TPD spectra following the adsorption of acetone (1.62 ML) on: a) clean- and b) pre-atomic-hydrogen-covered ($\theta_{\text{H,rel}} = 1$) Au(111) surfaces. All species were adsorbed onto the surface at 77 K. The heating rate was 1 K s^{-1} . Spectra (a) and (b) have the same scale for the y axis.

surface. Upon heating to 300 K with a ramp rate of 1 K s^{-1} , two desorption features appeared: second-layer desorption at 132 K and monolayer desorption at 155 K. With increasing acetone coverage, multilayer desorption created a distinct feature at 126–131 K (see the Supporting Information, Figure S1). Our TPD data was in excellent agreement with the results by Syomin and Koel.^[12] The signal from $m/z=58$ (parent mass of CH_3COCH_3) was also monitored to verify the desorption of CH_3COCH_3 .

On the pre-atomic-hydrogen-covered Au(111) surface, the thermal desorption spectrum of acetone changed significantly (Figure 1 b). Compared to the clean Au(111) surface, H atoms caused the desorption features to broaden. These interactions also shifted the monolayer desorption to a slightly higher temperature (158 K) and resulted in the appearance of two new desorption features at 195 and 210 K. However, no hydrogenated products (e.g., 2-propanol at $m/z=45$) were observed. Furthermore, no deuterated 2-propanol was generated from either $\text{H+CD}_3\text{COCD}_3$ or $\text{D+CH}_3\text{COCH}_3$. These results clearly indicated that, whereas there were noticeable interactions be-

[a] M. Pan, A. J. Brush, Prof. C. B. Mullins

Department of Chemical Engineering
University of Texas at Austin
Austin, TX 78703-0231 (USA)
Fax: (+1) 512-471-7060
E-mail: mullins@che.utexas.edu

[b] Dr. Z. D. Pozun, Prof. G. Henkelman

Department of Chemistry and Biochemistry
Institute for Computational Engineering and Sciences
University of Texas at Austin
Austin, TX 78712-0165 (USA)

Supporting information for this article is available on the WWW under <http://dx.doi.org/10.1002/cctc.201200311>.

tween acetone and hydrogen on the Au(111) surface, the catalytic activity was not high enough to initiate a reaction.

To assess gold as a hydrogenation catalyst for aldehydes as compared to ketones, we investigated the hydrogenation of propionaldehyde. Figure 2 shows TPD measurements of propionaldehyde on clean- (Figure 2a) and pre-adsorbed-hydro-

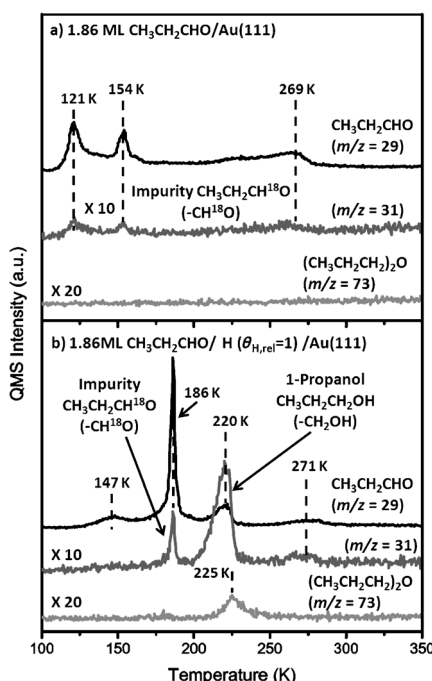


Figure 2. TPD spectra following the adsorption of propionaldehyde (1.82 ML) on: a) clean- and b) pre-atomic-hydrogen-covered ($\theta_{H,\text{rel}}=1$) Au(111) surfaces. All species were adsorbed onto the surface at 77 K. The heating rate was 1 K s^{-1} . Spectra (a) and (b) have the same scale for the y axis.

gen-covered (Figure 2 b) Au(111) surfaces. On the clean surface, 1.82 ML of propionaldehyde, which was represented by both the $m/z=29$ (CH_3CH_2 and CHO) and $m/z=31$ fragments (CH^{18}O ; from the natural abundance of ^{18}O), yielded multilayer- and monolayer-desorption features at 121 and 154 K, respectively. We also observed another desorption feature at 269 K, which was presumably associated with the polymerization of $\text{CH}_3\text{CH}_2\text{CHO}$ on the clean surface. The polymerization of aldehydes has been widely reported on many metal surfaces, including Ru,^[13] Au,^[14] Cu,^[15] and Pd.^[16] For more-detailed information on the desorption of propionaldehyde with various coverages, see the Supporting Information, Figure S2.

Figure 2b shows TPD measurements following the co-adsorption of 1.82 ML of $\text{CH}_3\text{CH}_2\text{CHO}$ and H atoms ($\theta_{H,\text{rel}}=1$) on a Au(111) surface at 77 K. With the co-adsorption of H atoms, the TPD-desorption spectra for propionaldehyde ($m/z=29$) showed several changes. Although the polymerization feature remained at 271 K, its integrated area was smaller than that of propionaldehyde on a clean Au(111) surface. In addition, we observed a small desorption feature at 147 K, a strong, sharp feature at 186 K, and a small feature at 220 K. The origins of these three peaks are unclear and more studies are required to understand them from a mechanistic point of view. The spec-

tra for $m/z=31$ (Figure 2b) displayed the expected small peaks at 186 K and 271 K, which corresponded to the natural abundance of CH^{18}O from the desorption of propionaldehyde (about 3% of $m/z=29$ as in Figure 2a). However, the desorption peak at 220 K for the $m/z=31$ curve was much larger than would be expected from natural abundance alone, thus indicating that 1-propanol was formed. We estimated that 90% of the $m/z=31$ desorption peak at about 220 K could be assigned to 1-propanol. The production of $\text{CH}_3\text{CH}_2\text{CH}_2\text{OH}$ was confirmed by the parent mass-fragment peak of 1-propanol, $m/z=60$, with the same shape and temperature (see the Supporting Information, Figure S3).

Comparison between the reactions of acetone and propionaldehyde with H atoms revealed a higher reactivity of $\text{CH}_3\text{CH}_2\text{CHO}$ on Au(111) surfaces and suggested chemoselectivity for the hydrogenation reaction on the gold surface. We used DFT calculations (for methods, see the Supporting Information) to understand the mechanisms on a molecular/atomic scale, similar to the study performed by Alcala and co-workers on a model Pt(111) surface.^[17] They found that the hydrogenation of propionaldehyde was more-favorable owing to its lower activation energy (0.54 eV) than acetone (0.76 eV). They asserted that the hydrogenation of the carbonyl-carbon atom is the first step, followed by the hydrogenation of the oxygen species.^[17] However, our DFT calculations (Figure 3) suggested different reaction pathways and mechanisms on a gold surface.

Acetone and propionaldehyde are structural isomers of one another. Acetone was calculated to be 0.33 eV lower in energy than propionaldehyde in the gas phase, owing to the higher thermodynamic stability of ketones compared to aldehydes. Our DFT calculations indicated that both species weakly chemisorbed onto the pre-atomic-hydrogen-covered gold surface (dispersion forces were not included in these calculations). Notably, whilst our DFT calculations indicated similar desorption energies for acetone and propionaldehyde, the TPD data for propionaldehyde (Figure 2b) indicated a significantly higher desorption energy than acetone (Figure 1b). This result is presumably due to the fact that these DFT calculations modeled single molecules and did not account for interactions between multiple surface species. Despite this discrepancy, our DFT calculations give valuable mechanistic insight into the chemoselectivity of gold by comparing the transition-state energies for the partially hydrogenated intermediates (see below).

The key step that anchors the molecules onto the surface is the hydrogenation of the carbonyl-oxygen atom. In each case, this process had a barrier of 0.2 eV. Following hydrogenation, the carbonyl-carbon atom became sp^3 hybridized and formed a covalent bond with a surface gold atom. This process is shown in Figure 3, which shows the displacement of the gold atom out of the surface owing to covalent interactions (Figure 3, panels 2A and 2B). Owing to the increased steric demands of the bulky methyl groups at the carbonyl-carbon positions in acetone, this protonation step was only exothermic by 0.1 eV. In contrast, hydrogenated propionaldehyde faced less steric interactions with the surface and the hydrogenation step was exothermic by over 0.4 eV.

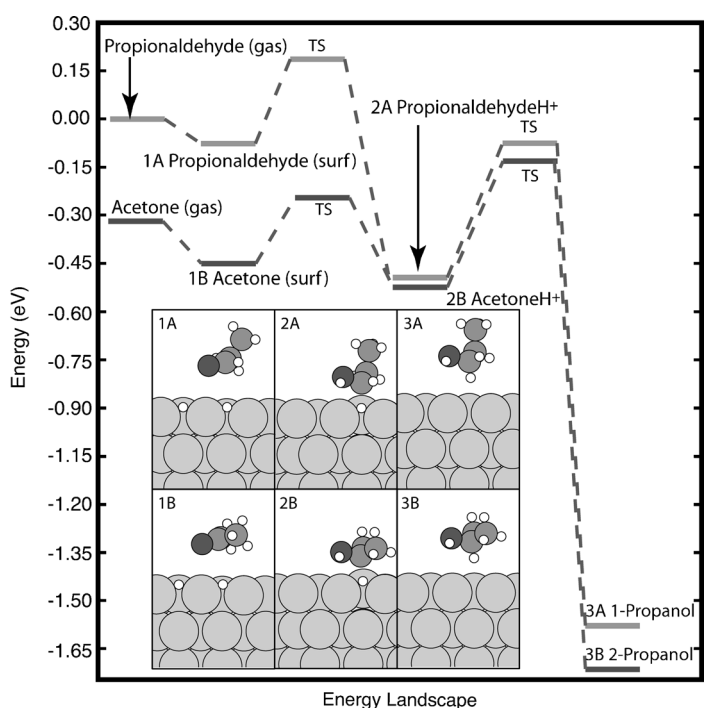


Figure 3. Energy diagram for the hydrogenation of acetone and propionaldehyde on a Au(111) surface.

Following the initial hydrogenation of the carbonyl-oxygen atom, the carbonyl-carbon atom is vulnerable to attack by surface hydrogen atoms. Although this reaction is highly exothermic in both cases, Figure 3 shows a possible explanation for the observance of 1-propanol and not 2-propanol. The barrier to hydrogenation of the carbonyl-carbon atom in propionaldehyde is significantly lower than the barrier to return the initial hydrogen atom to the surface. In contrast, acetone has a lower barrier for returning the initial hydrogen atom to the surface than that for hydrogenation of the carbonyl-carbon atom. Therefore, for the partially hydrogenated intermediates, the propionaldehyde intermediate is most likely to proceed to the fully hydrogenated 1-propanol, whereas the acetone intermediate is most likely to reverse back to give the adsorbed acetone.

An additional- and possibly more-important factor that favors the hydrogenation of propionaldehyde is the polymerization reaction. Comparison of Figure 1a and Figure 2a shows that propionaldehyde polymerizes on the clean surface, as indicated by the desorption peak at 269 K, but acetone does not. A similar phenomenon also occurred on the H-covered Au(111) surface. Hydrogenation of the carbonyl-oxygen atom activated the carbonyl-carbon atom, thereby allowing strong interactions with the oxygen atom of another molecule. As shown in the Supporting Information, Figure S4, polymerization with a second surface molecule was exothermic by 0.45 eV in propionaldehyde and endothermic by 0.3 eV in acetone. Thus, these polymerization reactions help to account for the increased susceptibility of propionaldehyde towards hydrogenation. The more-strongly bound polymer desorbed at a much-higher temperature, so the concentration of surface

molecules was higher at increased temperature such that the polymer may dissociate and undergo full hydrogenation. This result was also consistent with our observation that propionaldehyde showed a concomitant desorption feature with produced 1-propanol at 220 K (Figure 2b), which has also been observed in the hydrogenation of acetaldehyde on a Au(111) surface.^[14] In contrast, acetone did not polymerize; thus, desorption from the surface at lower temperatures remained favorable compared to hydrogenation.

As shown in Figure 2b, we also observed the desorption of di-*n*-propyl ether ($\text{CH}_3\text{CH}_2\text{CH}_2\text{OCH}_2\text{CH}_2\text{CH}_3$) from propionaldehyde on H-covered Au(111) surfaces. This species is represented by the curve for $m/z=73$, with a desorption feature that was centered at 225 K, and was verified by two other characteristic mass fragments at $m/z=43$ and 102 (see the Supporting Information, Figure S3); the fragment at $m/z=43$ was the most-abundant fragment and that at 102 was the parent mass. Figure 2a shows that the di-*n*-propyl ether did not originate from impurities in the reactant and strongly suggests that the compound was formed from a coupling reaction of propionaldehyde. Water-desorption was observed at 180 K and further supported the conclusion that the ether was formed through

a mechanism that was akin to the standard acid-catalyzed dehydration reaction in solution. A more-detailed study regarding the related reaction mechanisms is underway.

Isotope experiments were performed to further investigate the reaction mechanisms. First, we studied the hydrogenation reaction between $\text{CH}_3\text{CH}_2\text{CHO}$ and D atoms (Figure 4a), where 1.86 ML of propionaldehyde was adsorbed onto a deuterated Au(111) surface ($\theta_{\text{D},\text{rel}}=1$). The TPD spectrum for $m/z=33$ displayed a peak at 220 K, which was the same temperature as the desorption of 1-propanol in Figure 2b, and indicated the production of $\text{CH}_3\text{CH}_2\text{CHDOD}$, which was verified by the detection of the corresponding parent mass (62, not shown). In addition, we detected partially deuterated di-*n*-propyl ether ($\text{CH}_3\text{CH}_2\text{CHDOCHDCH}_2\text{CH}_3$) with a characteristic mass fragment at $m/z=75$ and a desorption peak at 225 K. Desorption peaks of the mass fragment $m/z=44$ and of the parent mass ($m/z=104$) were also observed (not shown).

In addition, these isotopic experiments provided insight into the kinetic isotope effect (KIE) on the surface reactions. Figure 4b shows the integrated areas under the desorption features of products 1-propanol ($m/z=31$ and 33) and di-*n*-propyl ether ($m/z=73$ and 75) as an indicator of their corresponding production in the H- and D-reaction systems. These results indicated a lower reactivity of deuterium for the surface reactions and showed values of 2.9 for the ratio of $m/z=31$ to $m/z=33$ (thus indicating the production of 1-propanol) and 1.3 for the ratio of $m/z=73$ to $m/z=75$ (thus indicating the production of the ether). Thus, we concluded that the reaction between propionaldehyde and H atoms was influenced by a KIE, which was comparably stronger for the hydrogenation of propionaldehyde than for the formation of di-*n*-propyl ether.

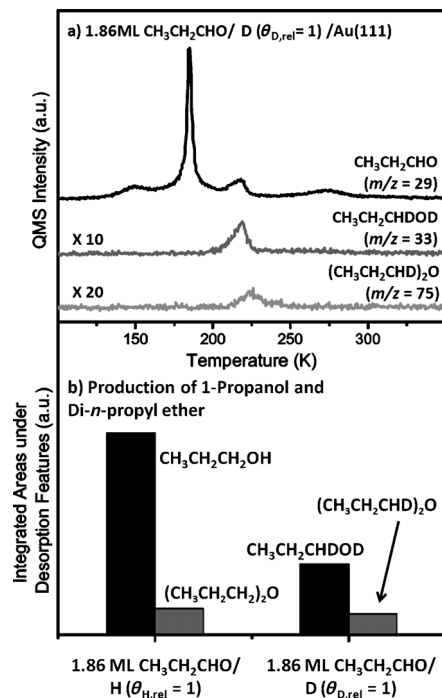


Figure 4. a) TPD spectra following the adsorption of propionaldehyde (1.82 ML) onto a pre-atomic-deuterium-covered ($\theta_{\text{D},\text{rel}} = 1$) Au(111) surface. b) Production of 1-propanol and di-n-propyl ether from the H- and D-covered surface. All species were adsorbed onto the surface at 77 K. The heating rate was 1 K s^{-1} .

In summary, acetone formed weak interactions with atomic H atoms on a Au(111) surface, as indicated by the TPD-desorption spectra. However, no hydrogenated product was observed. In contrast, the hydrogenation of propionaldehyde was detected by the production of 1-propanol. DFT calculations predicted similar energetic barriers for the initial hydrogenation reaction; however, the reverse reaction for acetone was favored over the final hydrogenation step. Conversely, the full hydrogenation reaction for propionaldehyde was favored over the reverse reaction. In addition, the polymerization of $\text{CH}_3\text{CH}_2\text{CHO}$ on a Au(111) surface was exothermic and may play a role in the hydrogenation reaction by increasing the surface concentration of propionaldehyde. Di-n-propyl ether can be generated by a coupling reaction of propionaldehyde on H-covered Au(111) and is likely generated in the reaction between surface intermediates and the produced alcohol. Deuteration-labeling experiments showed lowered reactivity for the production of both 1-propanol and di-n-propyl ether, thereby indicating the presence of a kinetic isotope effect.

Experimental Section

All of the experiments were performed in an ultrahigh-vacuum (UHV) supersonic-molecular-beam apparatus with a base pressure of 2×10^{-10} Torr.^[18] A quadrupole mass spectrometer (QMS) was used to monitor the gas-phase species that desorbed from the sample surface. H atoms were generated with a homemade electron-beam-heated device. For details of the experimental procedure, see the Supporting Information.

Acknowledgements

We thank the Department of Energy (DE-FG02-04ER15587) and the Welch Foundation (F-1436 for C.B.M., F-1601 for G.H.) for their support. M.P. acknowledges the William S. Livingston Fellowship, and Z.D.P. acknowledges the Dorothy B. Banks Fellowship for financial support.

Keywords: acetone · chemoselectivity · gold · hydrogenation · propionaldehyde

- [1] a) G. C. Bond, P. A. Sermon, G. Webb, D. A. Buchanan, P. B. Wells, *J. Chem. Soc. Chem. Commun.* **1973**, 444–445; b) W. S. Epling, G. B. Holflund, J. F. Weaver, S. Tsubota, M. Haruta, *J. Phys. Chem.* **1996**, *100*, 9929–9934; c) M. Haruta, *Catal. Today* **1997**, *36*, 153–166.
- [2] a) T. A. Baker, X. Y. Liu, C. M. Friend, *Phys. Chem. Chem. Phys.* **2011**, *13*, 34–46; b) J. Greeley, M. Mavrikakis, *J. Phys. Chem. B* **2005**, *109*, 3460–3471.
- [3] a) J. L. Gong, C. B. Mullins, *J. Am. Chem. Soc.* **2008**, *130*, 16458–16459; b) J. L. Gong, C. B. Mullins, *Acc. Chem. Res.* **2009**, *42*, 1063–1073; c) J. Kim, Z. Dohnálek, B. D. Kay, *J. Am. Chem. Soc.* **2005**, *127*, 14592–14593; d) B. K. Min, C. M. Friend, *Chem. Rev.* **2007**, *107*, 2709–2724; e) S. D. Senanayake, D. Stacchiola, P. Liu, C. B. Mullins, J. Hrbek, J. A. Rodriguez, *J. Phys. Chem. C* **2009**, *113*, 19536–19544.
- [4] a) J. Huang, T. Akita, J. Faye, T. Fujitani, T. Takei, M. Haruta, *Angew. Chem. Int. Ed.* **2009**, *48*, 8002–8006; *Angew. Chem. Int. Ed.* **2009**, *48*, 7862–7866; b) R. Si, M. Flytzani-Stephanopoulos, *Angew. Chem.* **2008**, *120*, 2926–2929; *Angew. Chem. Int. Ed.* **2008**, *47*, 2884–2887.
- [5] a) J. E. Bailie, H. A. Abdullah, J. A. Anderson, C. H. Rochester, N. V. Richardson, N. Hodge, J. G. Zhang, A. Burrows, C. J. Kiely, G. J. Hutchings, *Phys. Chem. Chem. Phys.* **2001**, *3*, 4113–4121; b) C. Milone, M. L. Tropeano, G. Gulino, G. Neri, R. Ingoglia, S. Galvagno, *Chem. Commun.* **2002**, 868–869; c) S. A. Nikolaev, V. V. Smirnov, *Gold Bull.* **2009**, *42*, 182–189; d) H. Sakurai, S. Tsubota, M. Haruta, *Appl. Catal. A* **1993**, *102*, 125–136.
- [6] a) B. Campo, M. Volpe, S. Ivanova, R. Touroude, *J. Catal.* **2006**, *242*, 162–171; b) T. V. Choudhary, C. Sivadinarayana, A. K. Datye, D. Kumar, D. W. Goodman, *Catal. Lett.* **2003**, *86*, 1–8; c) A. Corma, P. Serna, *Science* **2006**, *313*, 332–334; d) A. Corma, P. Serna, H. Garcia, *J. Am. Chem. Soc.* **2007**, *129*, 6358–6359.
- [7] a) B. Campo, C. Petit, M. A. Volpe, *J. Catal.* **2008**, *254*, 71–78; b) L. He, J. Ni, L. C. Wang, F. J. Yu, Y. Cao, H. Y. He, K. N. Fan, *Chem. Eur. J.* **2009**, *15*, 11833–11836.
- [8] R. Zheng, M. P. Humbert, Y. Zhu, J. G. Chen, *Catal. Sci. Technol.* **2011**, *1*, 638–643.
- [9] C. Mohr, H. Hofmeister, J. Radnik, P. Claus, *J. Am. Chem. Soc.* **2003**, *125*, 1905–1911.
- [10] P. Claus, *Appl. Catal. A* **2005**, *291*, 222–229.
- [11] B. Hammer, J. K. Norskov, *Nature* **1995**, *376*, 238–240.
- [12] D. Syomin, B. E. Koel, *Surf. Sci.* **2002**, *498*, 53–60.
- [13] M. A. Henderson, Y. Zhou, J. M. White, *J. Am. Chem. Soc.* **1989**, *111*, 1185–1193.
- [14] M. Pan, D. W. Flaherty, C. B. Mullins, *J. Phys. Chem. Lett.* **2011**, *2*, 1363–1367.
- [15] T. R. Bryden, S. J. Garrett, *J. Phys. Chem. B* **1999**, *103*, 10481–10488.
- [16] J. L. Davis, M. A. Bartea, *J. Am. Chem. Soc.* **1989**, *111*, 1782–1792.
- [17] R. Alcalá, J. Greeley, M. Mavrikakis, J. A. Dumesic, *J. Chem. Phys.* **2002**, *116*, 8973–8980.
- [18] a) J. E. Davis, S. G. Karseboom, P. D. Nolan, C. B. Mullins, *J. Chem. Phys.* **1996**, *105*, 8362–8375; b) J. E. Davis, P. D. Nolan, S. G. Karseboom, C. B. Mullins, *J. Chem. Phys.* **1997**, *107*, 943–952; c) M. Pan, S. Hoang, J. Gong, C. B. Mullins, *Chem. Commun.* **2009**, 7300–7302; d) M. Pan, S. Hoang, C. B. Mullins, *Catal. Today* **2011**, *160*, 198–203.

Received: May 12, 2012

Published online on July 17, 2012